Catalysis Letters (2020) 150:49–55
https://doi.org/10.1007/s10562-019-02952-y

# Plasmonic Oxidation of Glycerol Using Au/$TiO_2$ Catalysts Prepared by Sol-Immobilisation

**Laura Abis[1] · Nikolaos Dimitratos[1] · Meenakshisundaram Sankar[1] · Simon J. Freakley[1,2] · Graham J. Hutchings[1]**

Received: 16 July 2019 / Accepted: 9 August 2019 / Published online: 11 September 2019


## Abstract

Au nanoparticles supported on P25 $TiO_2$ (Au/$TiO_2$) were prepared by a facile sol-immobilisation method and investigated for the surface plasmon-assisted glycerol oxidation under base-free conditions. The Au/$TiO_2$ samples were characterized by UV–vis spectroscopy and transmission electron microscopy. Catalysts were prepared using polyvinyl alcohol as stabiliser as well as in the absence of polymer stabiliser. Both the conversion and the reaction selectivity are affected by the plasmon-assisted oxidation and there is an interplay between the presence of the stabiliser and the Au nanoparticle size.

## Graphic Abstract

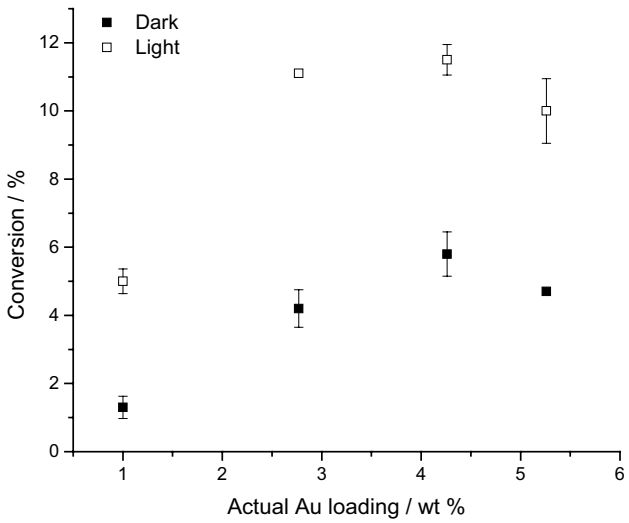


**Keywords** Gold · Plasmonic · Glycerol oxidation

## 1 Introduction

Glycerol is a potentially valuable by-product from the manufacture of biodiesel. Due to its high functionalisation, can be used as an important precursor for the fine chemicals industry [1–3]. The selective oxidation of glycerol has been extensively studied as a means of converting glycerol to potentially valuable products such as glyceric acid, tartronic acid and dihydroxyacetone [4, 5]. Supported Au catalysts have been shown to be very active for glycerol oxidation to

**Electronic supplementary material** The online version of this article (https://doi.org/10.1007/s10562-019-02952-y) contains supplementary material, which is available to authorized users.

✉ Graham J. Hutchings
hutch@cf.ac.uk

[1] School of Chemistry, Cardiff Catalysis Institute, Cardiff University, Main Building, Park Place, Cardiff CF10 3AT, UK

[2] Department of Chemistry, University of Bath, Claverton Down, Bath BA2 7AY, UK

glyceric acid under basic reaction conditions [6], and the high pH is required to activate the first hydroxyl group of glycerol. It has been found that catalysts that are active at high pH are typically inactive at neutral pH. In addition to the metal, the support can play a role and can be used to fine tune selectivity [7]. Indeed, although there are reports of base-free oxidation of glycerol with Au catalysts, these tended to utilise basic supports such as MgO but these are found to dissolve during the reaction in sufficient amounts to provide the basic environment which induces the selective oxidation [8]. Hence new approaches are required to observe catalysed base-free oxidation of glycerol.

Plasmonic photocatalysis is an emerging field that can offer a new strategy for the oxidation of glycerol. This relies on the plasmonic properties of noble metal nanoparticles, used to induce reactivity [9–17]. Among them, the gold-containing ones are of particular interest since they show a surface plasmon resonance (LSPR) falling in the visible range of the electromagnetic radiation, resulting in the possibility to harvest visible light to promote chemical reactions. Several works have been conducted for selective oxidation reactions of alcohols driven by plasmonic photocatalysis [18–26]. To date glycerol oxidation has been studied using traditional photocatalysts [27–31] and more recently Au catalysts [32, 33]. These earlier studies used monometallic Au catalysts prepared by deposition–precipitation, with a content of gold of typically > 5 wt%, and showed that base-free glycerol oxidation is indeed accelerated under visible light illumination [33]. Colloidal catalyst synthesis methods allow the control nanoparticle size, bimetallic nanoparticle composition and morphology (such as core shell particles) and control of nanoparticle shape in solution with greater flexibility than typical deposition methods. We wanted to explore the use of Au catalysts prepared using sol-immobilisation, as this method allows to obtain nanoparticles which can be < 5 nm in diameter with a reasonably narrow particle size distribution.

We aimed to examine catalysts containing lower Au concentrations, and in this paper we report the results for the plasmonic photocatalysis of glycerol using sol-immobilised $Au/TiO_2$ catalysts.

## 2 Experimental

### 2.1 Preparation of $Au/TiO_2$ Catalysts by Sol-Immobilisation

$Au/TiO_2$ catalysts were prepared by sol-immobilisation using polyvinyl alcohol (PVA) as a stabilising polymer. In a typical catalyst synthesis (1 g), an aqueous solution of $HAuCl_4 \cdot 3H_2O$ (0.8 mL, 12.5 mg Au/mL Sigma Aldrich, metal content ≥ 49.0%) was added to 400 mL of deionised water with stirring, followed by the addition of a polymer stabilizer (PVA 1 wt% aqueous solution (average molecular weight $M_W$ = 9000–10,000 g/mol, 80% hydrolysed), polymer/metal = 0.65 by weight). Subsequently, a freshly prepared solution of $NaBH_4$ (≥ 99.99%, Aldrich, 0.1 M) was added (mol $NaBH_4$/mol Au = 5) to form a red sol. After 30 min, the colloid was immobilised by adding 0.99 g of $TiO_2$ (P25 Aeroxide®, Evonik) together with concentrated $H_2SO_4$ (1 mL). After 1 h of continuous stirring, the slurry was filtered, and the catalyst was recovered by filtration and washed thoroughly with deionised water and dried (110 °C, 16 h). Catalysts were also prepared using the same procedure with no stabiliser present.

## 3 Glycerol Oxidation

Plasmonic oxidation of glycerol was carried out using a reactor design based on that used previously [33], and comprised a stainless steel custom designed autoclave reactor built by DG Innovation. The reactor consisted of two parts: a top, with a borosilicate window, equipped with inlet, outlet, thermocouple inlet, pressure gauge and pressure release valve; and a vessel where the reaction liner is located. A glass vial (15 mL) was placed in a Teflon jacket (2.5 cm diameter) and wrapped in aluminium foil to ensure both thermal contact and light reflection inside the reaction vessel. The maximum operating pressure of the reactor, determined by the presence of the window, is 11 bar. The maximum operating volume is 7.5 mL. Heating was provided by a heating mantle designed, connected to a control box (K39 Ascon Tecnologic, assembled by Elmatic, Cardiff). The light source is a 300 W lamp (USHIO) positioned inside a case and connected to a control box (ORIEL OPL-500). For all the experiments the IR radiation was removed from the output light by a water filter, and wavelengths below 420 nm were eliminated through a cut-off filter (Newport Stablife® Technology). The filtered light was focused on the top of the reactor through a 90° mirror placed at the end of the filters.

Plasmonic photocatalytic glycerol oxidation at pH 7 was carried out under dark and illuminated conditions with aqueous glycerol (5 mL, 0.05 M), catalyst (5 mg), Gly/Au = 130 molar ratio. The neutral pH is necessary as it is well known that the reaction of glycerol with gold catalysts is greatly accelerated by the presence of base and therefore in the present study we wanted to minimise any possible thermal reactions. After addition of the reactants the reactor was sealed, flushed with 5 bar $O_2$ five times and finally pressurised with $O_2$ (continuously supplied). The temperature was set to 90 °C and the experiment started when temperature in the heating mantle reached the selected value. Total reaction time was 3 h. After reaction, the reactor was rapidly quenched in an ice bath, the liner weighed and the slurry

collected, filtered through a micropore PTFE filter (0.25 µm) and directly injected to HPLC for analysis. Product analysis was carried out using an Agilent 1260 Infinity HPLC with a Metacarb 67H column with a 0.1 wt% solution of phosphoric acid as mobile phase.

### 3.1 Catalyst Characterisation

The plasmon resonance for the Au catalysts was determined using UV–visible spectroscopy. The metal content of the catalysts was determined inductively coupled plasma–mass spectrometry (Agilent 7900 ICP-MS) following digestion of the catalyst in aqua regia. Transmission electron microscopy analysis was performed using a JEOL 2100 microscope with a $LaB_6$ filament operating at 200 kV. Samples were prepared by dispersing the catalyst in ethanol and allowing a drop of suspension to evaporate on a lacey carbon film supported over a 300 mesh copper TEM grid.

## 4 Results and Discussion

### 4.1 Au/$TiO_2$ Catalysts Prepared Using PVA as Stabiliser

Au/$TiO_2$ catalysts (with nominal compositions 1, 3, 5, 7 wt%) were prepared by a sol–immobilisation method with and without PVA as the stabilising agent. The catalysts were analysed by ICP-MS and the measured Au contents are shown in Table 1 where it was observed that as the target metal loading was increased the actual metal loading deviated more from the target composition likely due to inefficient immobilisation of the Au sol with higher metal concentrations in the preparation.

The catalysts were tested for base-free glycerol oxidation under dark and illumination conditions (wavelengths above 420 nm with IR water filter in place) using constant catalyst (5 mg) and glycerol concentration (5 mL 0.05 M) and as a consequence the substrate/catalyst ratio changed for each Au concentration (Fig. 1) (Gly/Au molar ratio of 984, 357, 234, 186 with increasing metal content respectively). For all the samples, independent of the gold loading, an enhancement in the conversion under illumination was observed and a clear maximum is observed for the conversion under both dark and illuminated reaction conditions.

All of the samples showed a similar product distribution, with the selectivity under dark and illumination being predominantly to GA and DHA. Under illuminated conditions, the nominal 3, 5 and 7 wt% catalysts showed the formation of glycolic acid (Fig. 2), which was not detected

**Table 1** Au content of Au/$TiO_2$ catalysts prepared with and without PVA as stabilising agent

| Nominal Au wt% | Prepared with PVA Actual Au wt% | Prepared without PVA Actual Au wt% |
|---|---|---|
| 1 | 0.99 | 0.99 |
| 3 | 2.77 | 2.81 |
| 5 | 4.26 | 4.44 |
| 7 | 5.26 | 5.83 |

[a]Metal amount (wt%) determined by ICP

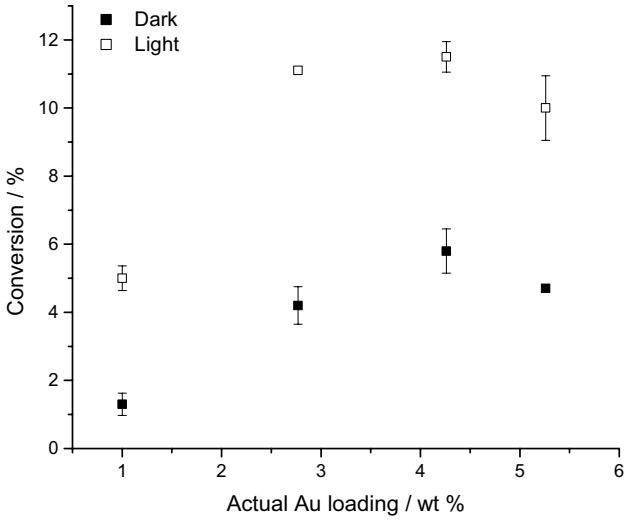


**Fig. 1** Conversion under illumination and dark conditions for the Au/$TiO_2$-PVA catalysts plotted versus the experimentally determined Au content of the catalyst

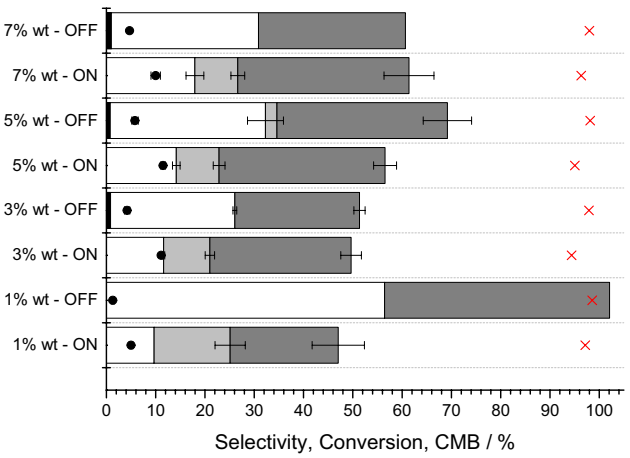


**Fig. 2** Catalytic activity of 1, 3, 5, 7 wt% Au/$TiO_2$–PVA. Reaction conditions: glycerol (5 mL, 0.05 M), catalyst (5 mg), 90 °C, 3 h, (1%) Gly/Au molar ratio = 984 (3%) Gly/Au molar ratio = 352 (5%) Gly/Au molar ratio = 234 (7%) Gly/Au molar ratio = 186. Key: filled circle glycerol conversion filled square pyruvic acid (PA) open square glyceric acid (GA) light grey coloured square glycolic acid (GLYA) dark grey coloured square dihydroxyacetone (DHA) × carbon mass balance (CMB); remaining product not shown is $CO_2$

in significant amounts under dark conditions. This might indicate a different or accelerated oxidation pathway occurring under illumination and this is considered to be due to the formation of $H_2O_2$ under these conditions as this is a well-known intermediate in photocatalysed reactions with Au resulting in C–C scission. Another feature common to all the samples is the production of $CO_2$, except for the 1% wt sample under dark reaction conditions, due to the low conversion observed. It is clear that the formation of $CO_2$ is a result of the sol-immobilised catalysts being more active than equivalent catalysts made by impregnation or precipitation which typically contain larger particles [33].

The catalysts were characterised by TEM (Fig. S1) and showed that the gold nanoparticles were well-dispersed on the support and displayed a very similar size distribution, averaging $2.8 \pm 0.7$ nm for all the samples. The catalysts were further characterised using UV–visible spectroscopy (Fig. S2). All the catalysts showed a plasmonic band at similar wavelength (around 540 nm), which is expected for the nanoparticle size observed by TEM. Also as expected, higher metal loading catalysts demonstrated a more intense plasmon resonance band. The similarity observed in the catalyst selectivity can therefore be explained by the similar morphologies of the catalysts with conversion determined by the metal loadings (Fig. 3).

The 3% wt $Au/TiO_2$ catalyst was investigated to determine the effect of the reaction time on conversion and selectivity under illumination (Fig. 4). Multiple experiments were carried out for selected times (45, 90, 120, 180 and 300 min). As expected, the conversion increases linearly with time of illumination showing that illumination does not induce significant deactivation, reaching 20% after 5 h. As the conversion increased with reaction the carbon mass balance decreased slightly possibly due to polymerisation of reaction products. Initially no glycolic acid was observed but this was observed at reaction longer than 45 min as a sequential oxidation product although DHA was observed in similar selectivity at all reaction times.

## 4.2 $Au/TiO_2$ Catalysts Prepared in the Absence of a Stabiliser

It has previously been shown that sol-immobilised catalysts active for glycerol oxidation under basic conditions can be prepared without the use of a stabilising [34]. Therefore an analogous series of catalysts with nominal Au loadings of 1, 3, 5, 7 wt% $Au/TiO_2$ were prepared without the use of a stabiliser in the sol-immobilisation preparation method. The Au content of these catalysts was determined using ICP analysis and the results shown in Table 1 show the concentrations are very similar to those analogous formulations prepared using PVA as stabiliser.

The catalysts were characterised by diffuse reflectance UV–Vis spectroscopic showed that all the samples present an absorption band corresponding to the plasmonic resonance, with values increasing with metal loading (Fig. S3). The shape and position of the plasmonic resonances change with increasing metal loading, with broader absorptions for the 3% and 5% samples and a red shift of the associated wavelengths. Also, both the signals of the 3% and 5% wt catalysts show a shoulder at higher wavelengths (more evident for the 5% wt sample) which might indicate a non-uniform resonance frequency, correspondent to a non-uniform particle size distribution [22]. TEM analysis carried out on the 1–7% wt $Au/TiO_2$-SF catalysts confirmed a broader size

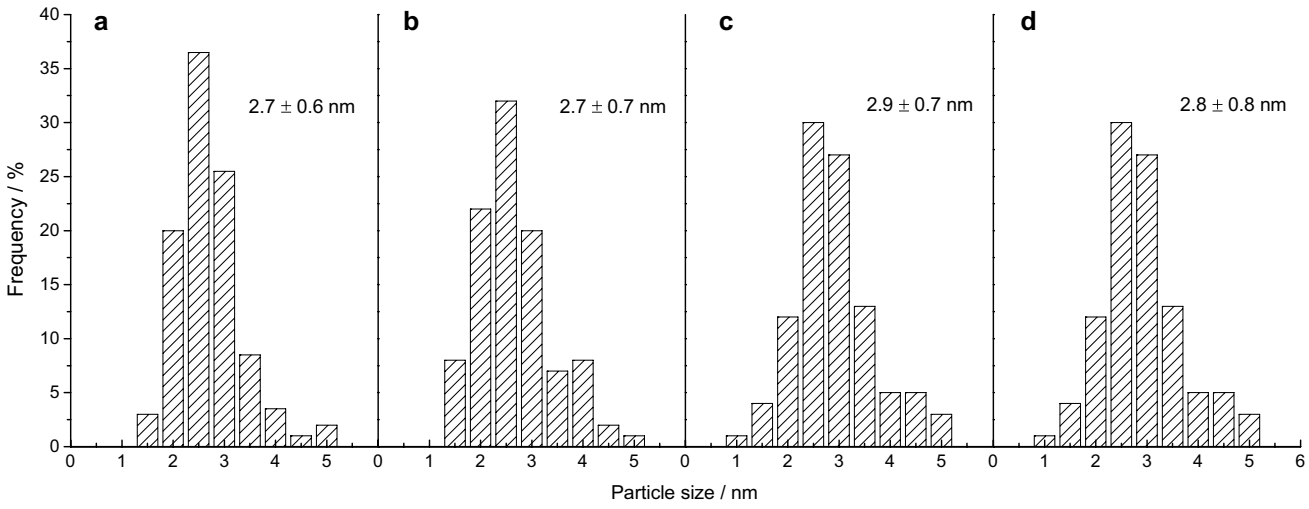


**Fig. 3** Nanoparticle size distribution for the 1, 3, 5, 7% (*a*, *b*, *c*, *d* respectively) wt% $Au/TiO_2$ catalysts derived by counting 100 nanoparticles from TEM images

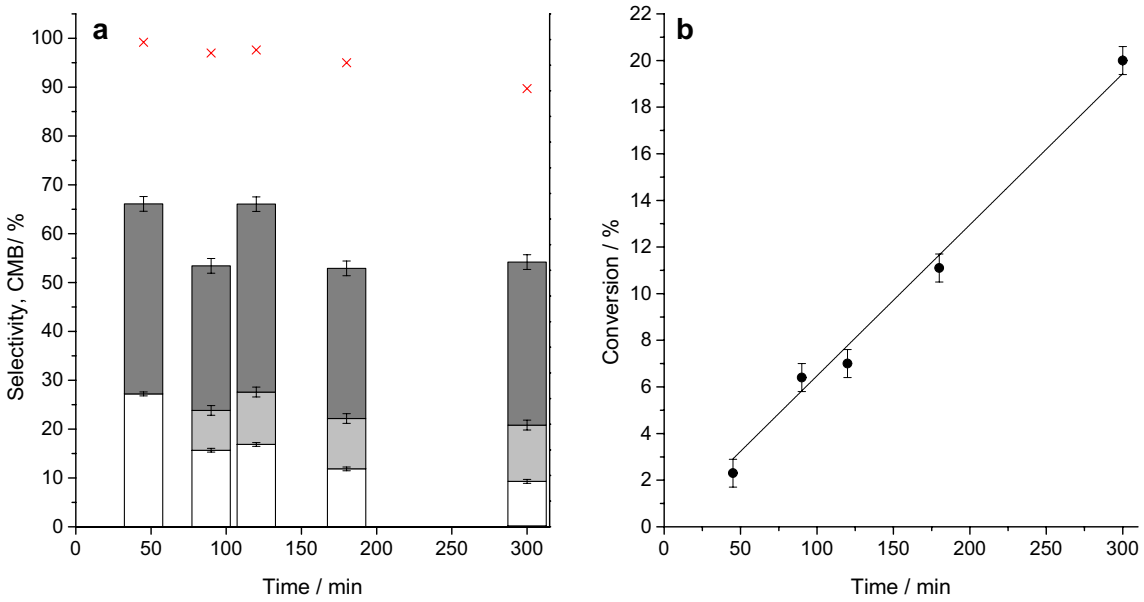


**Fig. 4** Effect on reaction time on **a** product selectivity and **b** glycerol conversion for 3% wt Au/$TiO_2$ under illumination. Reaction conditions: glycerol (5 mL 0.05 M), catalyst (5 mg), 90 °C, Gly/Au molar ratio = 357. Key: filled circle glycerol conversion filled square pyruvic acid (PA) open square glyceric acid (GA) light grey coloured square glycolic acid (GLYA) dark grey coloured square dihydroxyacetone (DHA) × carbon mass balance (CMB); remaining product not shown is $CO_2$

distribution and larger particle size at higher loadings (Figure S4 and Fig. 5).

Surprisingly, all the dried catalysts prepared by the stabiliser-free method were inactive, due in part to the larger particles sizes reducing the number of surface metal atoms significantly, suggesting that smaller nanoparticles are required for this reaction. The 7 wt% Au/$TiO_2$ catalyst showed a little activity under dark conditions, as shown in Fig. 6. When illuminated, its activity is switched on and it is as active as the equivalent catalyst prepared with stabiliser, having much smaller average particle size (7.3 nm vs 2.8 nm). This seems to suggest a pure dependence of the catalytic activity on the plasmonic resonance, with the catalytic system switched on or off under illumination for larger Au structures, which have a more intense plasmon resonance than sub 3 nm particles.

As the stabiliser may be influencing the catalyst activity, we investigated the effect of calcination on catalysts prepared with stabiliser as a method to burn away the residual organic species which are present on the surface. These can be detrimental for catalytic activity [35], but it is known

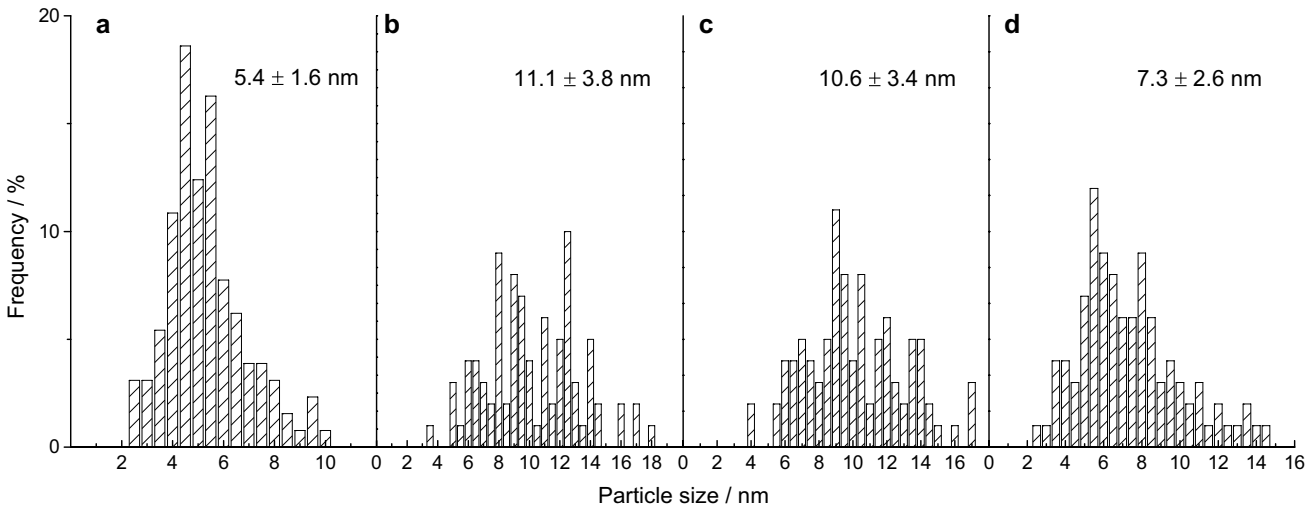


**Fig. 5** Nanoparticle size distribution for the 1, 3, 5, 7% wt (*a*, *b*, *c*, *d* respectively) Au/$TiO_2$–SF catalysts derived from TEM images

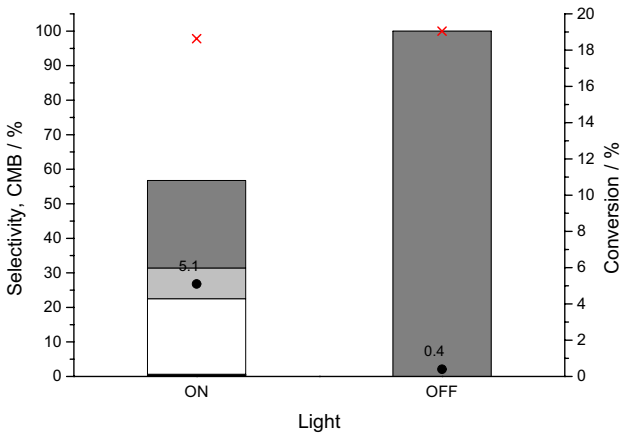


**Fig. 6** Glycerol oxidation using 7% wt Au/$TiO_2$-SF. Reaction conditions: glycerol (5 mL 0.05 M), catalyst (5 mg), 90 °C, 3 h. Gly/Au molar ratio = 140. Key: filled circle glycerol conversion filled square pyruvic acid (PA) open square glyceric acid (GA) light grey coloured square glycolic acid (GLYA) dark grey coloured square dihydroxyacetone (DHA) × carbon mass balance (CMB); remaining product not shown is $CO_2$

that the polymers can be removed effectively by calcination although this invariably increases the mean nanoparticle size. The 3% and the 5% wt Au/$TiO_2$ catalysts prepared using PVA were calcined at 500 °C in static air for 3 h which is known to effectively remove the polymer, and tested under the same conditions as the non-calcined catalysts [35]. The effect of calcination had a deleterious effect on the conversion (Fig. 7) but selectivity was not markedly affected. The loss of conversion is possibly due to the increase in particle size as shown by TEM (Figure S5) as the mean Au particle size increased from < 3 nm for the uncalcined catalysts to > 6.5 nm for the calcined catalysts. However, in all cases an enhancement under light illumination as still observed after calcination.

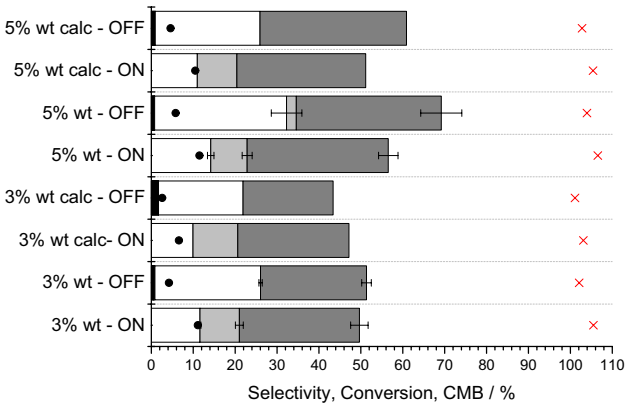


**Fig. 7** Calcination effect on the 3% and 5% wt Au/$TiO_2$–PVA catalysts, compared to the analogous dried catalysts. Reaction conditions: glycerol (5 mL, 0.05 M), catalyst (5 mg), 90 °C, 3 h, (3%) Gly/Au molar ratio = 330 (5%) Gly/Au molar ratio = 200. Key: filled circle glycerol conversion filled square pyruvic acid (PA) open square glyceric acid (GA) light grey coloured square glycolic acid (GLYA) dark grey coloured square dihydroxyacetone (DHA) × carbon mass balance (CMB); remaining product not shown is $CO_2$

## 5 Conclusions

These initial findings show that glycerol oxidation can be accelerated with visible light illumination under base free conditions using catalysts prepared by colloidal methods. Colloidal catalyst synthesis methods allow the control nanoparticle size, bimetallic nanoparticle composition and morphology (such as core shell particles) and control of nanoparticle shape in solution with greater flexibility than typical deposition methods. This provides new avenues for catalyst design based on optimising both the light absorption and catalyst properties in and new modes of operation in catalysts that can be switched on/off with light illumination.

## 6 Definitions

$$\text{Carbon conversion}\% = \frac{\text{moles of reactant converted (carbon)}}{\text{moles of fed reactant (carbon)}} \times 100$$

$$\text{Carbon selectivity}\% = \frac{\text{moles of product (carbon)}}{\text{moles of reactant converted (carbon)}} \times 100$$

$$\text{Carbon mass balance }\% = \frac{\Sigma\text{moles of liquid phase product (carbon)}}{\text{moles of fed reactant (carbon)}} \times 100$$

Moles of carbon are calculated by multiplying the moles of product/reactant by the number of carbons in the product/reactant). Unless otherwise stated, the results showed in the present paper are expressed as average of three experiments, and the associated error bars represent the standard deviation of each value.

**Acknowledgements** This work is supported by Cardiff University and the MAXNET Energy research consortium of the Max Planck Society and we thank Georgios Dodekatos and Harun Tüysüz for their advice and assistance with the reactor design.

## Compliance with Ethical Standards

**Conflict of interest** The authors declare no financial conflict of interest.

## References


1. Pagliaro M, Ciriminna R, Kimura H, Rossi M, Della Pina C (2007) Angew Chem Int Ed 46:4434–4440
2. Zhou CH, Beltramini JN, Fan YX, Lu GQ (2008) Chem Soc Rev 37:527–549
3. Behr A, Eilting J, Irawadi K, Leschinski J, Lindner F (2008) Green Chem 10:13–30
4. Katryniok B, Kimura H, Skrzynska E, Girardon JS, Fongarland P, Capron M, Ducoulombier R, Mimura N, Paul S, Dumeignil F (2011) Green Chem 13:1960–1979
5. Villa A, Dimitratos N, Chan-Thaw CE, Hammond C, Prati L, Hutchings GJ (2015) Acc Chem Res 48:1403–1412
6. Carrettin S, McMorn P, Johnston P, Griffin K, Hutchings GJ (2002) Chem Commun 696–697
7. Evans CD, Kondrat SA, Smith PJ, Manning TD, Miedziak PJ, Brett GL, Armstrong RD, Bartley JK, Taylor SH, Rosseinsky MJ, Hutchings GJ (2016) Faraday Discuss 188:427–450
8. Fu JL, He Q, Miedziak PJ, Brett GJ, Huang XY, Pattission S, Douthwaite M, Hutchings GJ (2018) Chem Eur J 24:2396–2402
9. Awazu K, Fujimaki M, Rockstuhl C, Tominaga J, Murakami H, Ohki Y, Yoshida N, Watanabe T (2008) J Am Chem Soc 130:1676–1680
10. Christopher P, Ingram DB, Linic S (2010) J Phys Chem C 114:9173–9177
11. Ingram DB, Christopher P, Bauer JL, Linic S (2011) ACS Catal 1:1441–1447
12. Christopher P, Xin HL, Marimuthu A, Linic S (2012) Nat Mater 11:1044–1050
13. Zhou X, Liu G, Yu J, Fan W (2012) J Mater Chem 22:21337–21354
14. Wang P, Huang BP, Dai Y, Whangbo MH (2012) Phys Chem Chem Phys 14:9813–9825
15. Kale MJ, Avanesian T, Christopher P (2014) ACS Catal 4:116–128
16. Khan MR, Chuan TW, Yousuf A, Chowdhury MNK, Cheng CK (2015) Catal Sci Technol 5:2522–2531
17. Dodekatos G, Schünemann S, Tüysüz H (2016) Top Curr Chem 371:215–252
18. Shiraishi Y, Hirai H (2008) J Photochem Photobiol C 9:157–170
19. Zhai WY, Xue SJ, Zhu AW, Luo YP, Tian Y (2011) ChemCatChem 3:127–130
20. Tanaka A, Hashimoto K, Kominami H (2011) Chem Commun 47:10446–10448
21. Tanaka A, Hashimoto K, Kominami H (2012) J Am Chem Soc 134:14526–14533
22. Tsukamoto D, Shiraishi Y, Sugano Y, Ichikawa S, Tanaka S, Hirai T (2012) J Am Chem Soc 134:6309–6315
23. Zhang XG, Ke XB, Zhu HY (2012) Chemistry A 18:8048–8056
24. Sugano Y, Shiraishi Y, Tsukamoto D, Ichikawa S, Tanaka S, Hirai T (2013) Angew Chem Int Ed 52:5295–5299
25. Sarina S, Zhu H, Jaatinen E, Xiao Q, Liu H, Jia J, Chen C, Zhao J (2013) J Am Chem Soc 135:5793–5801
26. Jolmenares JC, Lisowski P, Lomot D, Chernyayeva O, Lisovytskiy D (2015) Chem Sus Chem 8:1676–1685
27. Augugliaro V, El Nazer HAH, Loddo V, Mele A, Palmisano G, Palmisano L, Yurdakal S (2010) Catal Today 151:21–28
28. Minero C, Bedini A, Maurino V (2017) Appl Catal B 128:135–143
29. Zhang Y, Zhang N, Tang ZR, Xu YJ (2013) Chem Sci 4:1820–1824
30. Molinari A, Maldotti A, Bratovcic A, Magnacca G (2013) Catal Today 206:46–52
31. Hermes NA, Corsetti A, Lansarin MA (2014) Chem Lett 4:143–145
32. Schünemann S, Dodekatos G, Tüysüz H (2015) Chem Mater 27:7743–7750
33. Dodekatos G, Tüysüz H (2016) Catal Sci Technol 6:7307–7315
34. Abis L, Freakley SJ, Dodekatos G, Morgan DJ, Sankar M, Dimitratos N, He Q, Kiely CJ, Hutchings GJ (2017) ChemCatChem 9:2914–2918
35. Lopez-Sanchez JA, Dimitratos N, White S, Brett GL, Kesavan L, Miedziak PJ, Tiruvalam R, Jenkins RL, Carley AF, Knight DW, Kiely CJ, Hutchings GJ (2011) Nat Chem 3:551–556